
EVOLMPNN: PREDICTING MUTATIONAL EFFECT ON HOMOLOGOUS PROTEINS BY EVOLUTION ENCODING

Zhiqiang Zhong
Aarhus University
zzhong@cs.au.dk

Davide Mottin
Aarhus University
davide@cs.au.dk

February 22, 2024

ABSTRACT

Predicting protein properties is paramount for biological and medical advancements. Current protein engineering mutates on a typical protein, called the *wild-type*, to construct a family of homologous proteins and study their properties. Yet, existing methods easily neglect subtle mutations, failing to capture the effect on the protein properties. To this end, we propose EVOLMPNN, Evolution-aware Message Passing Neural Network, to learn evolution-aware protein embeddings. EVOLMPNN samples sets of anchor proteins, computes evolutionary information by means of residues and employs a differentiable evolution-aware aggregation scheme over these sampled anchors. This way EVOLMPNN can capture the mutation effect on proteins with respect to the anchor proteins. Afterwards, the aggregated evolution-aware embeddings are integrated with sequence embeddings to generate final comprehensive protein embeddings. Our model shows up to 6.4% better than state-of-the-art methods and attains $36\times$ inference speedup in comparison with large pre-trained models.

1 Introduction

Can we predict important properties of a protein by directly observing only the effect of a few mutations on such properties? This basic biological question [1, 2] has recently engaged the machine learning community due to the current availability of benchmark data [3, 4, 5]. Proteins are sequences of amino-acids (residues), which are the cornerstone of life and influence a number of metabolic processes, including diseases [6, 7]. For this reason, protein engineering stands at the forefront of modern biotechnology, offering a remarkable toolkit to manipulate and optimise existing proteins for a wide range of applications, from drug development to personalised therapy [8, 9, 10].

One fundamental process in protein engineering progressively mutates an initial protein, called the *wild-type*, to study the effect on the protein’s properties [11]. These mutations form a family of *homologous proteins* as in Figure 1. This process is appealing due to its cheaper cost compared to other methods and reduced time and risk [12, 13].

Yet, the way mutations affect the protein’s properties is not completely understood [14, 15, 16], as it depends on a number of chemical reactions and bonds among residues. For this reason, machine learning offers a viable alternative to model complex interactions among residues. Initial approaches employed *feature engineering* to capture protein’s evolution [17, 18]; yet, a manual approach is expensive and does not offer enough versatility. Advances in NLP and CV inspired the design of deep *protein sequence encoders* [19, 20, 21] and general purpose Protein Language Models (PLMs) that are pre-trained on large scale datasets of sequences. Notable PLMs include ProtBert [22], AlphaFold [23], TAPE Transformer [3] and ESM [24]. These models mainly rely on Multiple Sequence Alignments (MSAs) [25] to search on large databases of protein evolution. Nevertheless, this search process is insensitive to subtle yet crucial mutations and introduces additional computational burdens [26, 27].

To overcome the limitations of previous models, we propose EVOLMPNN, Evolution-aware Message Passing Neural Network, to predict the mutational effect on homologous proteins. Our fundamental assumption is that there are inherent correlations between protein properties and the sequence differences among them, as shown in Figure 1-(b). EVOLMPNN integrates both protein sequence and evolutionary information by identifying where and which mutations

occur on the target protein sequence, compared with known protein sequences and predicts the mutational effect on the target protein property. To avoid the costly *quadratic* pairwise comparison among proteins, we devise a theoretically grounded (see Section 4.6) *linear* sampling strategy to compute differences only among the proteins and a fixed number of anchor proteins (Section 4.2). We additionally introduce two extensions of our model, EVOLGNN and EVOLFORMER, to include available data on the relation among proteins (Section 4.5). The theoretical computation complexity of proposed methods are provided to guarantee their efficiency and practicality. We apply the proposed methods to three benchmark homologous protein property prediction datasets with nine splits. Empirical evaluation results (Section 5.1) show up to 6.7% Spearman’s ρ correlation improvement over the best performing baseline models, reducing the inference time by $36\times$ compared with pre-trained PLMs.

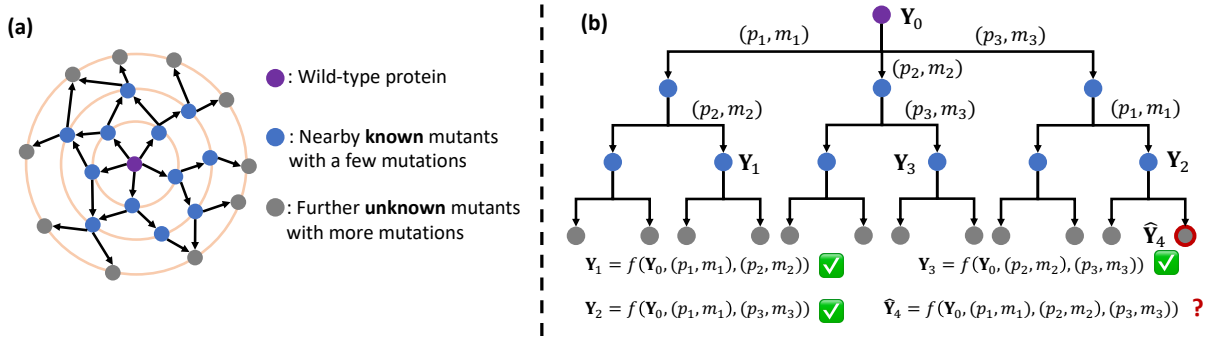


Figure 1: Protein property prediction on homologous protein family. (a) An example homologous protein family with labelled nearby mutants with few mutations. The task is to predict the label of unknown mutants with more mutations. (b) The evolutionary pattern for (a); (p_1, m_1) indicates the mutation m_1 at the p_1 -th position of the protein sequence.

2 Preliminary and Problem

In the protein engineering process, we first receive a *set of proteins* $\mathcal{M} = \{\mathcal{P}_i\}_{i=1,2,\dots,M}$ in which each protein can be associated with a label vector $\mathbf{Y}_i \in \mathbb{R}^\theta$ that describes its biomedical properties, *e.g.*, fitness, stability, fluorescence, solubility, etc. Each protein \mathcal{P}_i is a linear chain of *amino-acids* $\mathcal{P}_i = \{r_j\}_{j=1,2,\dots,N}$. While a protein sequence folds into specific 3D conformation to perform some biomedical functions, each amino-acid is considered as a *residue*. Residues are connected to one another by peptide bonds and can interact with each other by different chemical bounds [6]. In short, the function of a protein is mainly determined by the chemical interactions between residues. Since the 3D structure is missing in benchmark datasets [3, 4, 5], we assume no 3D protein information in this paper.

Homologous Protein Family. A set of protein sequences (\mathcal{M}) is a *homologous protein family* if there exists an ancestral protein \mathcal{P}_{WT} , called *wild-type*, such that any $\mathcal{P}_i \in \mathcal{M}$ is obtained by mutating \mathcal{P}_{WT} through substitution, deletion, insertion and truncation of residues [28]. As shown in Figure 1-(a), a homologous protein family can be organised together by representing their evolutionary relationships and Figure 1-(b) illustrates the detailed evolutionary patterns.

Research Problem. Protein engineering based on homologous proteins is a promising and essential direction for designing novel proteins of desired properties [29, 30]. Understanding the relation between protein sequence and property is one essential step. Practically, biologists perform experiments in the lab to label the property \mathbf{Y}_{TRAIN} of a set of protein $\mathcal{M}_{TRAIN} \subset \mathcal{M}$ and the follow-up task is predicting $\hat{\mathbf{Y}}_{TEST}$ of the rest proteins $\mathcal{M}_{TEST} \subset \mathcal{M}$. However, homologous proteins typically have similarities in their amino-acid sequences, structures, and functions due to their shared ancestry. Accurately predicting the homologous protein property by distinguishing these subtle yet crucial differences is still an open challenge.

3 Related Work

Feature Engineering. Besides conducting manual experiments in labs to measure protein properties, the basic solution is to design different feature engineering methods based on relevant biological knowledge, to extract useful information from protein sequence [31, 18, 32]. [4] introduce using Levenshtein distance [33] and BLOSUM62-score [34] relative to wild-type to design protein sequence features. In another benchmark work, [5] adopt another two typical protein sequence feature descriptors, *i.e.*, Dipeptide Deviation from Expected Mean (DDE) [17] and Moran correlation (Moran) [18]. For more engineering methods, refer to the comprehensive review [35].

Protein Representation Learning. In the last decades, empowered by the outstanding achievements of machine learning and deep learning, protein representation learning has revolutionised protein property prediction research. Early work along this line adopts the idea of word2vec [36] to protein sequences [37, 38]. To increase model capacity, deeper *protein sequence encoders* were proposed by the Computer Vision (CV) and Nature Language Processing (NLP) communities [19, 20, 21]. The latest works develop *Protein Language Models* (PLMs), which focus on employing deep sequence encoder models for protein sequences and are pre-trained on million- or billion-scale sequences. Well-known works include ProtBert [22], AlphaFold [23], TAPE Transformer [3] and ESM [24]. However, most existing work does not pay enough attention to these subtle yet crucial differences in homologous proteins. [24, 23] explore protein Multiple Sequence Alignments (MSAs) [39, 25] to capture the mutational effect. Nevertheless, the MSA searching process introduces additional computational burden and is insensitive to subtle but crucial sequence differences [26]. [27] indicate the shortcomings of MSAs on easily neglecting the presence of minor mutations, which can propagate errors to downstream protein sequence representation learning tasks. This paper also lies in this direction, we propose a novel solution for the challenging homologous protein property prediction tasks.

4 Framework

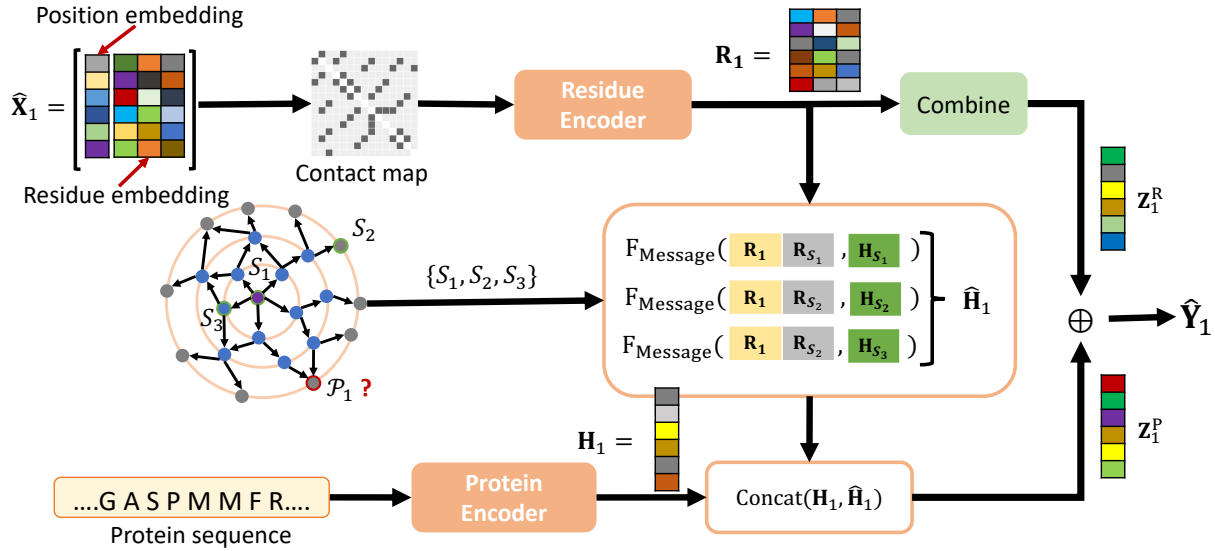


Figure 2: Our EVOLMPNN framework encodes protein mutations via a sapient combination of residue evolution and sequence encoding.

EVOLMPNN is a novel framework that integrates both protein sequence information and evolution information by means of residues. As a result, EVOLMPNN accurately predicts the mutational effect on homologous protein families. First, in Section 4.1, we introduce *embedding initialisation* for protein sequence and residues and the update module for residue embedding (Section 4.2). The *evolution encoding* in Section 4.3 is the cornerstone of the model that ameliorates protein embeddings. We conclude in Section 4.4 with the generation of *final proteins embeddings and model optimisation*. We complement our model with a theoretical analysis to motivate our methodology and a discussion of the computation complexity (Section 4.6). We additionally propose extended versions of EVOLMPNN that deal with available protein-protein interactions (Section 4.5).

4.1 Embedding Initialisation

Protein Sequence Embedding. Given a *set of proteins* $\mathcal{M} = \{\mathcal{P}_i\}_{i=1,2,\dots,M}$, we first adopt a (parameter-frozen) PLM model [40, 25]¹ as protein sequence encoder to initialise the protein sequence embedding (\mathbf{H}) for every protein \mathcal{P}_i , which include *macro* (i.e., protein sequence) level information as the primary embedding.

$$\mathbf{H} = \text{PLMENCODER}(\{\mathcal{P}_i\}_{i=1,2,\dots,M}), \quad (1)$$

where the obtained protein embedding $\mathbf{H} \in \mathbb{R}^{M \times d}$ and \mathbf{H}_i corresponds to each protein \mathcal{P}_i . Different encoders can extract information on various aspects, however, existing PLM models that rely on MSAs are not sensitive enough

¹We do not fine-tune PLM in this paper for efficiency consideration.

to capture the evolution pattern information in homologous protein families [26]. [27] systematically indicate the shortcomings of MSAs on easily neglecting the presence of minor mutations, which can propagate errors to downstream protein sequence representation learning tasks.

Residue Embedding. In order to properly capture the evolution information in homologous proteins, we delve into the residue level for *micro* clues. We adopt two residue embedding initialisation approaches, *i.e.*, one-hot encoding (Φ^{OH}) and pre-trained PLM encoder (Φ^{PLM}), to generate protein’s initial residue embeddings $\mathbf{X}_i = \{\mathbf{x}_j^i\}_{j=1,2,\dots,N}$, where $\mathbf{x}_j^i \in \mathbb{R}^d$. In particular, Φ^{OH} assigns each protein residue² with a binary feature vector \mathbf{x}_j^i , where $\mathbf{x}_{jb}^i = 1$ indicates the appearance of the b -th residue at \mathcal{P}_i ’s j -th position. By stacking N residues’ feature vectors into a matrix, we can obtain $\mathbf{X}_i \in \mathbb{R}^{N \times d}$. On the other hand, following the benchmark implementations [41], PLMENCODER can export residue embeddings similar to Eq. 1. Formally, Φ^{PLM} initialises protein residue embeddings as $\mathbf{X}_i = \text{PLMENCODER}(\{r_j\}_{j=1,2,\dots,N})$.

Position Embedding. Another essential component of existing PLM is the positional encoding, which was first proposed by [21]. This positional encoding effectively captures the relative structural information between entities and integrates it with the model [42]. In our case, correctly recording the position of each residue in the protein sequence plays an essential role in identifying each protein’s corresponding mutations. Because the same mutation that occurs at different positions may lead to disparate influences on protein property. Therefore, after initialising residue embeddings, we further apply positional embedding on each protein’s residues. We adopt a methodology that reminisces [43] that demonstrates the paramount importance of assigning each residue with a unique position embedding. As such, we randomly initialise a set of d position embeddings $\Phi^{\text{Pos}} \in \mathbb{R}^{N \times d}$. We denote the residue embedding empowered by position embedding as $\hat{\mathbf{X}}_i = \mathbf{X}_i \odot \Phi^{\text{Pos}}$.

4.2 Residue Embedding Update

The 3D protein folding depends on the strength of different chemical bonds between residues to maintain a stable 3D structure. Previous studies carefully designed residue contact maps to model the residue-residue interactions to learn effective residue embeddings [40, 44]. In this paper, we adopt the residue-residue interaction to update residue embeddings but eschew the requirement of manually designing the contact map. Instead, we assume the existence of an implicit fully connected residue contact map of each protein \mathcal{P}_i and implement the Transformer model [21, 45] to adaptively update residue embeddings. Denote $\mathbf{R}_i^{(\ell)}$ as the input to the $(\ell + 1)$ -th layer, with the first $\mathbf{R}_i^{(0)} = \hat{\mathbf{X}}_i$ be the input encoding. The $(\ell + 1)$ -th layer of residue embedding update module can be formally defined as follows:

$$\begin{aligned} \text{Att}_i^h(\mathbf{R}_i^{(\ell)}) &= \text{SOFTMAX}\left(\frac{\mathbf{R}_i^{(\ell)} \mathbf{W}_Q^{\ell,h} (\mathbf{R}_i^{(\ell)} \mathbf{W}_K^{\ell,h})^T}{\sqrt{d}}\right), \\ \hat{\mathbf{R}}_i^{(\ell)} &= \mathbf{R}_i^{(\ell)} + \sum_{h=1}^H \text{Att}_i^h(\mathbf{R}_i^{(\ell)}) \mathbf{R}_i^{(\ell)} \mathbf{W}_V^{\ell,h} \mathbf{W}_O^{\ell,h}, \\ \mathbf{R}_i^{(\ell+1)} &= \hat{\mathbf{R}}_i^{(\ell)} + \text{ELU}(\hat{\mathbf{R}}_i^{(\ell)} \mathbf{W}_1^\ell) \mathbf{W}_2^\ell, \end{aligned} \quad (2)$$

where $\mathbf{W}_O^{\ell,h} \in \mathbb{R}^{d_H \times d}$, $\mathbf{W}_Q^{\ell,h}$, $\mathbf{W}_K^{\ell,h}$, $\mathbf{W}_V^{\ell,h} \in \mathbb{R}^{d \times d_H}$, $\mathbf{W}_1^\ell \in \mathbb{R}^{d \times r}$, $\mathbf{W}_2^\ell \in \mathbb{R}^{d_t \times d}$, H is the number of attention heads, d_H is the dimension of each head, d_t is the dimension of the hidden layer, ELU [46] is an activation function, and $\text{Att}_i^h(\mathbf{R}_i^{(\ell)})$ refers to as the attention matrix. After each Transformer layer, we add a normalisation layer *i.e.*, LayerNorm [47], to reduce the over-fitting problem proposed by [21]. After stacking L_r layers, we obtain the final residue embeddings as $\mathbf{R}_i = \mathbf{R}_i^{(L_r)}$.

4.3 Evolution Encoding

In homologous protein families, all proteins are mutants derived from a common wild-type protein \mathcal{P}_{WT} with different numbers and types of mutations. In this paper, we propose to capture the evolutionary information via the following assumption.

Assumption 1 (Protein Property Relevance). *Assume there is a homologous protein family \mathcal{M} and a function F_{DIFF} can accurately distinguish the mutations on mutant \mathcal{P}_i compared with any \mathcal{P}_j as $F_{\text{DIFF}}(\mathcal{P}_i, \mathcal{P}_j)$. For any target protein \mathcal{P}_i , its property \mathbf{Y}_i can be predicted by considering 1) its sequence information \mathcal{P}_i ; 2) $F_{\text{DIFF}}(\mathcal{P}_i, \mathcal{P}_j)$ and the property of \mathcal{P}_j , *i.e.*, \mathbf{Y}_j . Shortly, we assume there exists a function f that maps $\mathbf{Y}_i \leftarrow f(F_{\text{DIFF}}(\mathcal{P}_i, \mathcal{P}_j), \mathbf{Y}_j)$.*

²There are 20 different amino-acid residues commonly found in proteins

Motivated by Assumption 1, we take both protein sequence and the mutants difference $F_{\text{DIFF}}(\mathcal{P}_i, \mathcal{P}_j)$ to accurately predict the protein property. To encode the protein sequence, we employ established tools described in Section 4.1. Here instead, we describe the evolution encoding to realise the function of $F_{\text{DIFF}}(\mathcal{P}_i, \mathcal{P}_j)$.

The naïve solution to extract evolutionary patterns in a homologous family is constructing a complete phylogenetic tree [48] based on the mutation distance between each protein pair. Yet, finding the most parsimonious phylogenetic tree is NP-hard [49].

To address the aforementioned problems, we propose an *anchor-based protein evolution encoding* method. Specifically, denote $\mathbf{H}_i^{(\ell)}$ as the input to the $(\ell + 1)$ -th block and define $\mathbf{H}_i^{(0)} = \mathbf{H}_i$. The evolution localisation encoding of the $(\ell + 1)$ -th layer contains the following key components: (i) k anchor protein $\{\mathcal{P}_{S_i}\}_{i=1,2,\dots,k}$ selection. (ii) Evolutionary information encoding function F_{DIFF} that computes the difference between residues of each protein and those of the anchor protein, and target protein’s evolutionary information is generated by summarising the obtained differences:

$$\mathbf{d}_{ij} = \text{COMBINE}(\mathbf{R}_i - \mathbf{R}_{S_j}), \quad (3)$$

where COMBINE can be implemented as differentiable operators, such as, CONCATENATE, MAX POOL MEAN POOL and SUM POOL; here we use the MEAN POOL to obtain $\mathbf{d}_{ij} \in \mathbb{R}^d$. (iii) Message computation function F_{MESSAGE} that combines protein sequence feature information of two proteins with their evolutionary differences. We empirically find that the simple element-wise product between $\mathbf{H}_j^{(\ell)}$ and \mathbf{d}_{ij} attains good results

$$F_{\text{MESSAGE}}(i, j, \mathbf{H}_j^{(\ell)}, \mathbf{d}_{ij}) = \mathbf{H}_j^{(\ell)} \odot \mathbf{d}_{ij}, \quad (4)$$

(iv) Aggregate messages from k anchors and combine them with protein’s embedding as follow:

$$\hat{\mathbf{H}}_i^{(\ell)} = \text{COMBINE}(\{F_{\text{MESSAGE}}(i, j, \mathbf{H}_j^{(\ell)}, \mathbf{d}_{ij})\}_{j=1,2,\dots,k}), \quad (5)$$

$$\mathbf{H}_i^{(\ell+1)} = \text{CONCAT}(\mathbf{H}_i^{(\ell)}, \hat{\mathbf{H}}_i^{(\ell)})\mathbf{W}^\ell, \quad (6)$$

where $\mathbf{W}^\ell \in \mathbb{R}^{2d \times d}$ transform concatenated vectors to the hidden dimension. After stacking L_p layers, we obtain the final protein sequence embedding $\mathbf{Z}_i^p = \mathbf{H}_i^{(L_p)}$.

4.4 Final Embedding and Optimisation

After obtaining protein \mathcal{P}_i ’s residue embeddings \mathbf{R}_i and sequence embedding \mathbf{Z}_i^p , we summarise its residue embeddings as a vector $\mathbf{Z}_i^r = \text{MEAN POOL}(\mathbf{R}_i)$. The final protein embedding summarises the protein sequence information and evolution information as the comprehensive embedding $\mathbf{Z}_i = \text{CONCAT}(\mathbf{Z}_i^p, \mathbf{Z}_i^r)$ and the final prediction is computed as $\hat{\mathbf{Y}}_i = \mathbf{Z}_i \mathbf{W}^{\text{FINAL}}$ where $\mathbf{W}^{\text{FINAL}} \in \mathbb{R}^{d \times \theta}$, θ is the number of properties to predict. Afterwards, we adopt a simple and common strategy, similar to [5], to solve the protein property prediction tasks. Specifically, we adopt the MSE Loss (\mathcal{L}) to measure the correctness of model predictions on training samples against ground truth labels. The objective of learning the target task is to optimise model parameters to minimise the loss \mathcal{L} on this task. The framework of EVOLMPNN is summarised in Algorithm 1 in Appendix A.

4.5 Extensions on Observed Graph

EVOLMPNN does not leverage any information from explicit geometry among proteins, where each protein only communicates with randomly sampled anchors (Section 4.3). However, it is often possible to have useful structured data $G = (\mathcal{M}, \mathbf{A})$ that represents the relation between protein-protein by incorporating specific domain knowledge [50].³ Therefore, here we introduce EVOLGNN, an extension of EVOLMPNN on the possibly observed protein interactions.

EVOLGNN. We compute the evolution information as Eq. 3. The evolution information can be easily integrated into the pipeline of message-passing neural networks, as an additional structural coefficient [51]:

$$\begin{aligned} \mathbf{m}_a^{(\ell)} &= \text{AGGREGATE}^{\mathcal{N}}(\{\mathbf{A}_{ij}, \underbrace{\mathbf{d}_{ij}}_{\text{Evol. info.}}, \mathbf{H}_j^{(\ell-1)} \mid j \in \mathcal{N}(i)\}), \\ \mathbf{m}_i^{(\ell)} &= \text{AGGREGATE}^{\mathcal{I}}(\{\mathbf{A}_{ij}, \underbrace{\mathbf{d}_{ij}}_{\text{Evol. info.}} \mid j \in \mathcal{N}(i)\}) \mathbf{H}_i^{(\ell-1)}, \\ \mathbf{H}_i^{(\ell)} &= \text{COMBINE}(\mathbf{m}_a^{(\ell)}, \mathbf{m}_i^{(\ell)}), \end{aligned} \quad (7)$$

³Available contact map describes residue-residue interactions can be easily integrated as relational bias of Transformer [45] as we used in Section 4.2.

where $\text{AGGREGATE}^{\mathcal{N}}(\cdot)$ and $\text{AGGREGATE}^{\mathcal{T}}(\cdot)$ are two parameterised functions. $\mathbf{m}_a^{(\ell)}$ is a message aggregated from the neighbours $\mathcal{N}(i)$ of protein \mathcal{P}_i and their structure (\mathbf{A}_{ij}) and evolution (\mathbf{d}_{ij}) coefficients. $\mathbf{m}_i^{(\ell)}$ is an updated message from protein \mathcal{P}_i after performing an element-wise multiplication between $\text{AGGREGATE}^{\mathcal{T}}(\cdot)$ and $\mathbf{H}_i^{(\ell-1)}$ to account for structural and evolution effects from its neighbours. After, $\mathbf{m}_a^{(\ell)}$ and $\mathbf{m}_i^{(\ell)}$ are combined together to obtain the update embedding $\mathbf{H}_i^{(\ell)}$.

EVOLFORMER. Another extension relies on pure Transformer structure, which means the evolution information of \mathcal{M} can be captured by every protein. The evolution information can be integrated into the pipeline of Transformer, as additional information to compute the attention matrix:

$$\text{Att}^h(\mathbf{H}^{(\ell)}) = \text{SOFTMAX}\left(\frac{\mathbf{H}^{(\ell)}\mathbf{W}_Q^{\ell,h}(\mathbf{H}^{(\ell)}\mathbf{W}_K^{\ell,h})^{\text{T}}}{\sqrt{d}} + \underbrace{\text{MEAN POOL}(\{\mathbf{R}_i\}_{i=1,2,\dots,M})}_{\text{Evol. info.}}\right), \quad (8)$$

Other follow-up information aggregation and feature vector update operations are the same as the basic Transformer pipeline, as described in Eq. 2.

4.6 Theoretical Analysis

Anchor Selection. Inspired by [52], we adopt Bourgain’s Theorem [53] to guide the random anchor number (k) of the evolution encoding layer. Briefly, support by a constructive proof (Theorem 2 [54]) of Bourgain Theorem (Theorem 1), only $k = O(\log^2 M)$ anchors are needed to ensure the resulting embeddings are guaranteed to have low distortion (Definition 1), in a given metric space $(\mathcal{M}, F_{\text{DIST}})$. EVOLMPNN can be viewed as a generalisation of the embedding method of Theorem 2, where $F_{\text{DIST}}(\cdot)$ is generalised via message passing functions (Eq 3-Eq. 6). Therefore, Theorem 2 offers a theoretical guide that $O(\log^2 M)$ anchors are needed to guarantee low distortion embedding. Following this principle, EVOLMPNN choose $k = \log^2 M$ random anchors, denoted as $\{S_j\}_{j=1,2,\dots,\log^2 M}$, and we sample each protein in \mathcal{M} independently with probability $\frac{1}{2^j}$. Detailed discussion and proof refer to Appendix B.

Complexity Analysis. The computation costs of EVOLMPNN, EVOLGNN, and EVOLFORMER come from residue encoding and evolution encoding, since the protein sequence and residue feature initialisation have no trainable parameters. The residue encoder introduces the complexity of $O(MN)$ following an efficient implementation of NodeFormer [45]. In the evolution encoding, EVOLMPNN performs communication between each protein and $\log^2 M$ anchors, which introduces the complexity of $O(M \log^2 M)$; EVOLGNN performs communication between each protein and K neighbours with $O(KM)$ complexity; EVOLFORMER performs communication between all protein pairs, which introduces the complexity of $O(M)$, following the efficient implement, NodeFormer. In the end, we obtain the total computation complexity of EVOLMPNN - $O((N + \log^2 M)M)$, EVOLGNN - $O((N + K)M)$ and EVOLFORMER - $O((N + 1)M)$.

5 Experimental Study

In this section, we empirically study the performance of EVOLMPNN. We validate our model on three benchmark homologous protein family datasets and evaluate the methods on nine data splits to consider comprehensive practical use cases. Our experiments comprise a comprehensive set of state-of-the-art methods from different categories. We additionally demonstrate the effectiveness of two extensions of our model, EVOLGNN and EVOLFORMER, with different input features. We conclude our analysis studying the influence of some hyper-parameters and investigating the performance of EVOLMPNN on high mutational mutants.

Datasets and Splits. We perform experiments on benchmark datasets of several important protein engineering tasks, including AAV, GB1 and Fluorescence, and generate three splits on each dataset. Data statistics are summarised in Table 1. The split λ -VS-REST indicates that we train models on wild-type protein and mutants of no more than λ mutations, while the rest are assigned to test. The split LOW-VS-HIGH indicates that we train models on sequences with target value scores equal to or below wild-type, while the rest are assigned to test. For more details refer to Appendix C.

Baselines. As baseline models, we consider methods in four categories. First, we selected four *feature engineer* methods, *i.e.*, Levenshtein [4], BLOSUM62 [4], DDE [17] and Moran [18]. Second, we select four *protein sequence encoder* models, *i.e.*, LSTM [19], Transformer [3], CNN [3] and ResNet [20]. Third, we select four *pre-trained PLM models*, *i.e.*, ProtBert [55], ESM-1b [24], ESM-1v [25] and ESM-2 [56]. In the end, we select four *GNN-based methods* which can utilise available graph structure, *i.e.*, GCN [57], GAT [58], GraphTransformer [59] and NodeFormer [45].

Table 1: Datasets splits, and corresponding statistics; if the split comes from a benchmark paper, we report the corresponding citation.

Landscape	Split	# Total	#Train	#Valid	#Test
AAV [14]	2-vs-REST [4]	82,583	28,626	3,181	50,776
	7-vs-REST [4]	82,583	63,001	7,001	12,581
	LOW-vs-HIGH [4]	82,583	42,791	4,755	35,037
GB1 [16]	2-vs-REST [4]	8,733	381	43	8,309
	3-vs-REST [4]	8,733	2,691	299	5,743
	LOW-vs-HIGH [4]	8,733	4,580	509	3,644
Fluorescence [15]	2-vs-REST	54,025	12,712	1,413	39,900
	3-vs-REST [5]	54,025	21,446	5,362	27,217
	LOW-vs-HIGH	54,025	44,082	4,899	5,044

Implementation. We follow the PEER benchmark settings⁴, including train and test pipeline, model optimisation and evaluation method (evaluation is Spearman’s ρ metric), adopted in [5] to make sure the comparison fairness. For the baselines, including feature engineer, protein sequence encoder and pre-trained PLM, we adopt the implementation provided by benchmark Torchdrug [41] and the configurations reported in [5]. For the GNN-based baselines, which require predefined graph structure and protein features, we construct K -NN graphs [60], with $K = \{5, 10, 15\}$, and report the best performance. As features, we use the trained sequence encoder, which achieves better performance, used also in our method. In addition, we adopt ESM-1b as the residue encoder on GB1 dataset and adopt One-Hot encoding on AAV and Fluorescence datasets to speed up the training process. All experiments are conducted on two NVIDIA GeForce RTX 3090 GPUs with 24 GB memory, and we report the mean performance of three runs with different random seeds. We present more details in Appendix D. Note that we do not report results that take more than 48 hours due to our limited computation resources.

5.1 Effectiveness

Table 2: Quality in terms Spearman’s ρ correlation with target value. NA indicates a non-applicable setting. * Used as a feature extractor with pre-trained weights frozen. † Results reported in [4, 5]. - Can not complete the training process within 48 hours on our devices. Top-2 performances of each split are marked as **bold** and underline.

Category	Model	Dataset								
		AAV			GB1			Fluorescence		
		2-vs-R.	7-vs-R.	L.-vs-H.	2-vs-R.	3-vs-R.	L.-vs-H.	2-vs-R.	3-vs-R.	L.-vs-H.
Feature Engineer	Levenshtein	0.578	0.550	0.251	0.156	-0.069	-0.108	0.466	0.054	0.011
	BLOSUM62	NA	NA	NA	0.128	0.005	-0.127	NA	NA	NA
	DDE	0.649 [†]	0.636	0.158	0.445 [†]	0.816	0.306	0.690	0.638 [†]	0.159
	Moran	0.437 [†]	0.398	0.069	0.069 [†]	0.589	0.193	0.445	0.400 [†]	0.046
Protein Seq. Encoder	LSTM	0.125 [†]	0.608	0.308	-0.002 [†]	-0.002	-0.007	0.256	0.494 [†]	0.207
	Transformer	0.681 [†]	0.748	0.304	0.271 [†]	0.877	0.474	0.250	0.643 [†]	0.161
	CNN	0.746 [†]	0.730	<u>0.406</u>	0.502 [†]	0.857	0.515	<u>0.805</u>	<u>0.682[†]</u>	0.249
	ResNet	0.739 [†]	0.733	0.223	0.133 [†]	0.542	0.396	0.594	0.636 [†]	<u>0.243</u>
Pre-trained PLM	ProtBert	0.794 [†]	-	-	0.634 [†]	0.866	0.308	0.451	0.679 [†]	-
	ProtBert*	0.209 [†]	0.507	0.277	0.123 [†]	0.619	0.164	0.403	0.339 [†]	0.161
	ESM-1b	0.821 [†]	-	-	0.704 [†]	<u>0.878</u>	0.386	0.804	0.679 [†]	-
	ESM-1b*	0.454 [†]	0.573	0.241	0.337 [†]	0.605	0.178	0.528	0.430 [†]	0.091
	ESM-1v*	0.533	0.580	0.171	0.359	0.632	0.180	0.562	0.563	0.070
	ESM-2*	0.475	0.581	0.199	0.422	0.632	0.189	0.501	0.511	0.084
GNN-based Methods	GCN	0.824	0.730	0.361	0.745	0.865	0.466	0.755	0.677	0.198
	GAT	0.821	0.741	0.369	<u>0.757</u>	0.873	0.508	0.768	0.667	0.208
	GraphTransf.	0.827	0.749	0.389	0.753	0.876	0.548	0.780	0.678	0.231
	NodeFormer	<u>0.827</u>	0.741	0.393	<u>0.757</u>	0.877	0.543	0.794	0.677	0.213
Ours	EVOLMPNN	0.835	0.757	0.433	0.768	0.881	0.584	0.809	0.684	0.228

EVOLMPNN outperforms all baselines on 8 of 9 splits. Table 2 summarises performance comparison on AAV, GB1 and Fluorescence datasets. EVOLMPNN achieves new state-of-the-art performance on most splits of three datasets, with up to 6.7% improvements to baseline methods. This result vindicates the effectiveness of our proposed design to capture evolution information for homologous protein property prediction. Notably, GNN-based methods that utilise manually constructed graph structure do not enter top-2 on 9 splits and two Transformer structure models,

⁴https://github.com/DeepGraphLearning/PEER_Benchmark

i.e., GraphTransformer and NodeFormer, often outperform such methods. It can be understood since homology graph construction is a challenging biomedical task [26], the simple K -NN graph construction is not an effective solution.

Large-scale PLM models are dominated by simple models. Surprisingly, we find that smaller models, such as CNN and ResNet, can outperform large ESM variants pre-trained on million- and billion-scale sequences. For instance, ESM-1v has about 650 million parameters and is pre-trained on around 138 million UniRef90 sequences [25]. Yet, CNN outperforms ESM-1v on three splits of Fluorescence dataset. This indicates the necessity of designs targeting specifically the crucial homologous protein engineering task.

Table 3: Results on GB1 datasets (metric: Spearman’s ρ) of our proposed methods, with different residue embeddings. Top-2 performances of each split marked as **bold** and underline.

Model	Split		
	2-vs-R.	3-vs-R.	L.-vs-H.
Best Baseline	0.757	0.878	0.548
EVOLMPNN (Φ^{OH})	0.766	0.877	0.553
EVOLGNN (Φ^{OH})	0.764	0.866	0.536
EVOLFORMER (Φ^{OH})	0.764	0.868	0.537
EVOLMPNN (Φ^{PLM})	0.768	0.881	0.584
EVOLGNN (Φ^{PLM})	<u>0.767</u>	<u>0.879</u>	<u>0.581</u>
EVOLFORMER (Φ^{PLM})	0.766	0.879	0.575

Our proposed extension models outperform all baselines on GB1 dataset. We performed additional experiments on GB1 datasets to investigate the performance of two extended models, *i.e.*, EVOLGNN and EVOLFORMER and study the influence of different residue embedding initialisation methods. The results summarised in Table 3 evince that EVOLMPNN outperforms the other two variants in three splits, and all our proposed models outperform the best baseline. This result confirms the effectiveness of encoding evolution information for homologous protein property prediction. Besides, the models adopting the PLM encoding Φ^{PLM} achieve better performance than those using the one-hot encoding Φ^{OH} . From this experiment, we conclude that residue information provided by PLM helps to capture protein’s evolution information.

5.2 Analysis of Performance

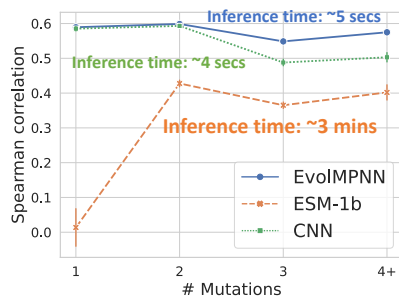
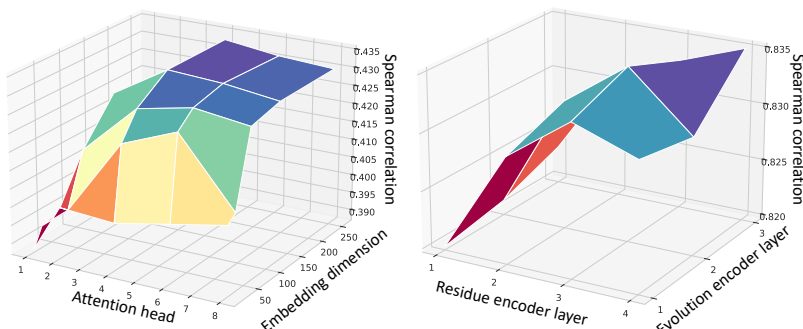


Figure 3: Performance on protein groups of different numbers of mutations, with the LOW-VS-HIGH split and avg. epoch inference time on GB1 dataset.



(a) #Attention Heads & #Embedding Dimension (b) Residue & Evolution Encoder #Layers

Figure 4: EVOLMPNN performance on AAV’s 2-VS-REST (a) and LOW-VS-HIGH (b) splits, with different hyper-parameters.

The performance of EVOLMPNN comes from its superior predictions on high mutational mutants. For the LOW-VS-HIGH split of GB1 dataset, we group the test proteins into 4 groups depending on their number of mutations. Next, we compute three models, including EVOLMPNN, ESM-1b (fine-tuned PLM model) and CNN (best baseline), prediction performances on each protein group and present the results in Figure 3. EVOLMPNN outperforms two baselines in all 4 protein groups. Notably, by demonstrating EVOLMPNN’s clear edge in groups of no less than 3 mutations, we confirm the generalisation effectiveness from low mutational mutants to high mutational mutants. **As per inference time**, EVOLMPNN and CNN require similar inference time (≈ 5 secs), $36\times$ faster than ESM-1b (≈ 3 mins).

Influence of hyper-parameter settings on EVOLMPNN. We present in Figure 4 a group of experiments to study the influence of some hyper-parameters on EVOLMPNN, including the number of attention heads, embedding dimension

and the number of layers of residue encoder and evolution encoder. EVOLMPNN exhibits stable performance on different hyper-parameter settings.

6 Conclusion and Future Work

We propose Evolution-aware Message Passing Neural Network (EVOLMPNN), that integrates both protein sequence information and evolution information by means of residues to predict the mutational effect on homologous proteins. Empirical and theoretical studies show that EVOLMPNN and its extended variants (EVOLGNN and EVOLFORMER) achieve outstanding performance on several benchmark datasets while retaining reasonable computation complexity. In future work, we intend to incorporate 3D protein structure information towards general-purpose homologous protein models.

Acknowledgments

This work is supported by the Horizon Europe and Innovation Fund Denmark under the Eureka, Eurostar grant no E115712 - AAVanguard.

References

- [1] James A Wells. Additivity of mutational effects in proteins. *Biochemistry*, 29(37):8509–8517, 1990. 1
- [2] Douglas M Fowler and Stanley Fields. Deep mutational scanning: a new style of protein science. *Nature methods*, 11(8):801–807, 2014. 1
- [3] Roshan Rao, Nicholas Bhattacharya, Neil Thomas, Yan Duan, Xi Chen, John F. Canny, Pieter Abbeel, and Yun S. Song. Evaluating protein transfer learning with TAPE. In *Proceedings of the 2019 Annual Conference on Neural Information Processing Systems (NeurIPS)*, pages 9686–9698, 2019. 1, 2, 3, 6
- [4] Christian Dallago, Jody Mou, Kadina E. Johnston, Bruce J. Wittmann, Nicholas Bhattacharya, Samuel Goldman, Ali Madani, and Kevin Yang. FLIP: benchmark tasks in fitness landscape inference for proteins. In *Proceedings of the 2021 Annual Conference on Neural Information Processing Systems (NeurIPS)*, 2021. 1, 2, 6, 7, 14
- [5] Minghao Xu, Zuobai Zhang, Jiarui Lu, Zhaocheng Zhu, Yangtian Zhang, Chang Ma, Runcheng Liu, and Jian Tang. PEER: A comprehensive and multi-task benchmark for protein sequence understanding. In *Proceedings of the 2022 Annual Conference on Neural Information Processing Systems (NeurIPS)*, 2022. 1, 2, 5, 7, 14
- [6] Linus Pauling, Robert B Corey, and Herman R Branson. The structure of proteins: two hydrogen-bonded helical configurations of the polypeptide chain. *Proceedings of the National Academy of Sciences*, 37(4):205–211, 1951. 1, 2
- [7] Trey Ideker and Roded Sharan. Protein networks in disease. *Genome Research*, 18(4):644–652, 2008. 1
- [8] Kevin M Ulmer. Protein engineering. *Science*, 219(4585):666–671, 1983. 1
- [9] Paul J Carter. Introduction to current and future protein therapeutics: a protein engineering perspective. *Experimental cell research*, 317(9):1261–1269, 2011. 1
- [10] Ethan C Alley, Grigory Khimulya, Surojit Biswas, Mohammed AlQuraishi, and George M Church. Unified rational protein engineering with sequence-based deep representation learning. *Nature methods*, 16(12):1315–1322, 2019. 1
- [11] Roland J Siezen, William M de Vos, Jack AM Leunissen, and Bauke W Dijkstra. Homology modelling and protein engineering strategy of subtilases, the family of subtilisin-like serine proteinases. *Protein Engineering, Design and Selection*, 4(7):719–737, 1991. 1
- [12] Meng Wang, Tong Si, and Huimin Zhao. Biocatalyst development by directed evolution. *Bioresource Technology*, 115:117–125, 2012. 1
- [13] Martin KM Engqvist and Kersten S Rabe. Applications of protein engineering and directed evolution in plant research. *Plant Physiology*, 179(3):907–917, 2019. 1
- [14] Drew H Bryant, Ali Bashir, Sam Sinai, Nina K Jain, Pierce J Ogden, Patrick F Riley, George M Church, Lucy J Colwell, and Eric D Kelsic. Deep diversification of an aav capsid protein by machine learning. *Nature Biotechnology*, 39(6):691–696, 2021. 1, 7, 14

- [15] Karen S Sarkisyan, Dmitry A Bolotin, Margarita V Meer, Dinara R Usmanova, Alexander S Mishin, George V Sharonov, Dmitry N Ivankov, Nina G Bozhanova, Mikhail S Baranov, Onuralp Soylemez, et al. Local fitness landscape of the green fluorescent protein. *Nature*, 533(7603):397–401, 2016. 1, 7, 14
- [16] Nicholas C Wu, Lei Dai, C Anders Olson, James O Lloyd-Smith, and Ren Sun. Adaptation in protein fitness landscapes is facilitated by indirect paths. *Elife*, 5:e16965, 2016. 1, 7, 14
- [17] Vijayakumar Saravanan and Namasivayam Gautham. Harnessing computational biology for exact linear b-cell epitope prediction: a novel amino acid composition-based feature descriptor. *Omics: a journal of integrative biology*, 19(10):648–658, 2015. 1, 2, 6
- [18] Zhi-Ping Feng and Chun-Ting Zhang. Prediction of membrane protein types based on the hydrophobic index of amino acids. *Journal of Protein Chemistry*, 19:269–275, 2000. 1, 2, 6
- [19] Sepp Hochreiter and Jürgen Schmidhuber. Long short-term memory. *Neural Computation*, 1997. 1, 3, 6
- [20] Fisher Yu, Vladlen Koltun, and Thomas A. Funkhouser. Dilated residual networks. In *Proceedings of the 2017 Conference on Computer Vision and Pattern Recognition (CVPR)*, pages 636–644. IEEE, 2017. 1, 3, 6
- [21] Ashish Vaswani, Noam Shazeer, Niki Parmar, Jakob Uszkoreit, Llion Jones, Aidan N. Gomez, Lukasz Kaiser, and Illia Polosukhin. Attention is all you need. In *Proceedings of the 2017 Annual Conference on Neural Information Processing Systems (NIPS)*, pages 5998–6008, 2017. 1, 3, 4
- [22] Nadav Brandes, Dan Ofer, Yam Peleg, Nadav Rappoport, and Michal Linial. Proteinbert: a universal deep-learning model of protein sequence and function. *Bioinformatics*, 38(8):2102–2110, 2022. 1, 3
- [23] John Jumper, Richard Evans, Alexander Pritzel, Tim Green, Michael Figurnov, Olaf Ronneberger, Kathryn Tunyasuvunakool, Russ Bates, Augustin Žídek, Anna Potapenko, et al. Highly accurate protein structure prediction with alphafold. *Nature*, 596(7873):583–589, 2021. 1, 3
- [24] Alexander Rives, Joshua Meier, Tom Sercu, Siddharth Goyal, Zeming Lin, Jason Liu, Demi Guo, Myle Ott, C Lawrence Zitnick, Jerry Ma, et al. Biological structure and function emerge from scaling unsupervised learning to 250 million protein sequences. *Proceedings of the National Academy of Sciences*, 118(15):e2016239118, 2021. 1, 3, 6
- [25] Joshua Meier, Roshan Rao, Robert Verkuil, Jason Liu, Tom Sercu, and Alexander Rives. Language models enable zero-shot prediction of the effects of mutations on protein function. In *Proceedings of the 2021 Annual Conference on Neural Information Processing Systems (NeurIPS)*, pages 29287–29303, 2021. 1, 3, 6, 8
- [26] William R Pearson. An introduction to sequence similarity (“homology”) searching. *Current Protocols in Bioinformatics*, 42(1):3–1, 2013. 1, 3, 4, 8
- [27] Maria Chatzou, Cedrik Magis, Jia-Ming Chang, Carsten Kemena, Giovanni Bussotti, Ionas Erb, and Cedric Notredame. Multiple sequence alignment modeling: methods and applications. *Briefings in Bioinformatics*, 17(6):1009–1023, 2016. 1, 3, 4
- [28] Helga Ochoterena, Alexander Vrijdaghs, Erik Smets, and Regine Claßen-Bockhoff. The search for common origin: homology revisited. *Systematic Biology*, 68(5):767–780, 2019. 2
- [29] Po-Ssu Huang, Gustav Oberdorfer, Chunfu Xu, Xue Y Pei, Brent L Nannenga, Joseph M Rogers, Frank DiMaio, Tamir Gonen, Ben Luisi, and David Baker. High thermodynamic stability of parametrically designed helical bundles. *science*, 346(6208):481–485, 2014. 2
- [30] Robert A Langan, Scott E Boyken, Andrew H Ng, Jennifer A Samson, Galen Dods, Alexandra M Westbrook, Taylor H Nguyen, Marc J Lajoie, Zibo Chen, Stephanie Berger, et al. De novo design of bioactive protein switches. *Nature*, 572(7768):205–210, 2019. 2
- [31] Petr Klein, Minoru Kanehisa, and Charles DeLisi. The detection and classification of membrane-spanning proteins. *Biochimica et Biophysica Acta (BBA)-Biomembranes*, 815(3):468–476, 1985. 2
- [32] Jiawei Wang, Bingjiao Yang, Jerico Revote, Andre Leier, Tatiana T Marquez-Lago, Geoffrey Webb, Jiangning Song, Kuo-Chen Chou, and Trevor Lithgow. Possum: a bioinformatics toolkit for generating numerical sequence feature descriptors based on pssm profiles. *Bioinformatics*, 33(17):2756–2758, 2017. 2
- [33] Yujian Li and Bi Liu. A normalized levenshtein distance metric. *IEEE Transactions on Pattern Analysis and Machine Intelligence (TPAMI)*, 29(6):1091–1095, 2007. 2
- [34] Sean R Eddy. Where did the blosum62 alignment score matrix come from? *Nature Biotechnology*, 22(8):1035–1036, 2004. 2
- [35] David Lee, Oliver Redfern, and Christine Orengo. Predicting protein function from sequence and structure. *Nature Reviews Molecular Cell Biology*, 8(12):995–1005, 2007. 2

- [36] Tomas Mikolov, Ilya Sutskever, Kai Chen, Gregory S. Corrado, and Jeffrey Dean. Distributed representations of words and phrases and their compositionality. In *Proceedings of the 2013 Annual Conference on Neural Information Processing Systems (NIPS)*, pages 3111–3119, 2013. 3
- [37] Ying Xu, Jiangning Song, Campbell Wilson, and James C Whisstock. Phoscontext2vec: a distributed representation of residue-level sequence contexts and its application to general and kinase-specific phosphorylation site prediction. *Scientific Reports*, 8(1):8240, 2018. 3
- [38] Marıa Katherine Mejıa-Guerra and Edward S Buckler. A k-mer grammar analysis to uncover maize regulatory architecture. *BMC Plant Biology*, 19(1):1–17, 2019. 3
- [39] Roshan Rao, Jason Liu, Robert Verkuil, Joshua Meier, John F. Canny, Pieter Abbeel, Tom Sercu, and Alexander Rives. MSA transformer. In *Proceedings of the 2021 International Conference on Machine Learning (ICML)*, volume 139, pages 8844–8856. PMLR, 2021. 3
- [40] Roshan Rao, Joshua Meier, Tom Sercu, Sergey Ovchinnikov, and Alexander Rives. Transformer protein language models are unsupervised structure learners. In *Proceedings of the 2021 International Conference on Learning Representations (ICLR)*, 2021. 3, 4
- [41] Zhaocheng Zhu, Chence Shi, Zuobai Zhang, Shengchao Liu, Minghao Xu, Xinyu Yuan, Yangtian Zhang, Junkun Chen, Huiyu Cai, Jiarui Lu, Chang Ma, Runcheng Liu, Louis-Pascal A. C. Xhonneux, Meng Qu, and Jian Tang. Torchdrug: A powerful and flexible machine learning platform for drug discovery. *CoRR*, abs/2202.08320, 2022. 4, 7
- [42] Chengxuan Ying, Tianle Cai, Shengjie Luo, Shuxin Zheng, Guolin Ke, Di He, Yanming Shen, and Tie-Yan Liu. Graph random neural networks for semi-supervised learning on graphs. In *Proceedings of the 2021 Annual Conference on Neural Information Processing Systems (NeurIPS)*, pages 28877–28888, 2021. 4
- [43] Anian Ruoss, Gregoire Deletang, Tim Genewein, Jordi Grau-Moya, Robert Csordas, Mehdi Bennani, Shane Legg, and Joel Veness. Randomized positional encodings boost length generalization of transformers. In *Proceedings of the 2023 Annual Meeting of the Association for Computational Linguistics (ACL)*, pages 1889–1903. ACL, 2023. 4
- [44] Ziqi Gao, Chenran Jiang, Jiawen Zhang, Xiaosen Jiang, Lanqing Li, Peilin Zhao, Huanming Yang, Yong Huang, and Jia Li. Hierarchical graph learning for protein–protein interaction. *Nature Communications*, 14(1):1093, 2023. 4
- [45] Qitian Wu, Wentao Zhao, Zenan Li, David P. Wipf, and Junchi Yan. Nodeformer: A scalable graph structure learning transformer for node classification. In *Proceedings of the 2022 Annual Conference on Neural Information Processing Systems (NeurIPS)*, pages 27387–27401, 2022. 4, 5, 6
- [46] Djork-Arne Clevert, Thomas Unterthiner, and Sepp Hochreiter. Fast and accurate deep network learning by exponential linear units (elus). *CoRR*, abs/1511.07289, 2015. 4
- [47] Jimmy Lei Ba, Jamie Ryan Kiros, and Geoffrey E Hinton. Layer normalization. *CoRR*, abs/1607.06450, 2016. 4
- [48] Walter M Fitch and Emanuel Margoliash. Construction of phylogenetic trees: a method based on mutation distances as estimated from cytochrome c sequences is of general applicability. *Science*, 155(3760):279–284, 1967. 5
- [49] David Sankoff. Minimal mutation trees of sequences. *SIAM Journal on Applied Mathematics*, 28(1):35–42, 1975. 5
- [50] Zhiqiang Zhong, Anastasia Barkova, and Davide Mottin. Knowledge-augmented graph machine learning for drug discovery: A survey from precision to interpretability. *CoRR*, abs/2302.08261, 2023. 5
- [51] Asiri Wijesinghe and Qing Wang. A new perspective on "how graph neural networks go beyond weisfeiler-lehman?". In *Proceedings of the 2022 International Conference on Learning Representations (ICLR)*, 2022. 5
- [52] Jiaxuan You, Rex Ying, and Jure Leskovec. Position-aware graph neural networks. In *Proceedings of the 2019 International Conference on Machine Learning (ICML)*, volume 97, pages 7134–7143. PMLR, 2019. 6, 13
- [53] Jean Bourgain. On lipschitz embedding of finite metric spaces in hilbert space. *Israel Journal of Mathematics*, 52:46–52, 1985. 6, 13, 14
- [54] Nathan Linial, Eran London, and Yuri Rabinovich. The geometry of graphs and some of its algorithmic applications. *Combinatorica*, 15:215–245, 1995. 6, 14
- [55] Ahmed Elnaggar, Michael Heinzinger, Christian Dallago, Ghalia Rehawi, Yu Wang, Llion Jones, Tom Gibbs, Tamas Feher, Christoph Angerer, Martin Steinegger, Debsindhu Bhowmik, and Burkhard Rost. Prottrans: Toward

- understanding the language of life through self-supervised learning. *IEEE Transactions on Pattern Analysis and Machine Intelligence (TPAMI)*, 44(10):7112–7127, 2022. 6
- [56] Zeming Lin, Halil Akin, Roshan Rao, Brian Hie, Zhongkai Zhu, Wenting Lu, Nikita Smetanin, Robert Verkuil, Ori Kabeli, Yaniv Shmueli, et al. Evolutionary-scale prediction of atomic-level protein structure with a language model. *Science*, 379(6637):1123–1130, 2023. 6
- [57] Thomas N. Kipf and Max Welling. Semi-supervised classification with graph convolutional networks. In *Proceedings of the 2017 International Conference on Learning Representations (ICLR)*, 2017. 6
- [58] Petar Velickovic, Guillem Cucurull, Arantxa Casanova, Adriana Romero, Pietro Lio, and Yoshua Bengio. Graph attention networks. In *Proceedings of the 2018 International Conference on Learning Representations (ICLR)*, 2018. 6
- [59] Yunsheng Shi, Zhengjie Huang, Shikun Feng, Hui Zhong, Wenjing Wang, and Yu Sun. Masked label prediction: Unified message passing model for semi-supervised classification. In *Proceedings of the 2021 International Joint Conferences on Artificial Intelligence (IJCAI)*, pages 1548–1554, 2021. 6
- [60] David Eppstein, Michael S Paterson, and F Frances Yao. On nearest-neighbor graphs. *Discrete & Computational Geometry*, 17:263–282, 1997. 7
- [61] LH Vandenberghe, JM Wilson, and G Gao. Tailoring the aav vector capsid for gene therapy. *Gene Therapy*, 16(3):311–319, 2009. 14
- [62] Hildegard Büning, Anke Huber, Liang Zhang, Nadja Meumann, and Ulrich Hacker. Engineering the aav capsid to optimize vector–host-interactions. *Current Opinion in Pharmacology*, 24:94–104, 2015. 14
- [63] Christopher Barnes, Olivia Scheideler, and David Schaffer. Engineering the aav capsid to evade immune responses. *Current opinion in biotechnology*, 60:99–103, 2019. 14
- [64] A Elisabeth Sauer-Eriksson, Gerard J Kleywegt, Mathias Uhlén, and T Alwyn Jones. Crystal structure of the c2 fragment of streptococcal protein g in complex with the fc domain of human igg. *Structure*, 3(3):265–278, 1995. 14
- [65] U Sjöbring, L Björck, and W Kastern. Streptococcal protein g. gene structure and protein binding properties. *Journal of Biological Chemistry*, 266(1):399–405, 1991. 14
- [66] Roger Y Tsien. The green fluorescent protein. *Annual Review of Biochemistry*, 67(1):509–544, 1998. 14

A Algorithm

Algorithm 1: The framework of EVOLMPNN

Input: Protein set $\mathcal{M} = \{\mathcal{P}_i\}_{i=1,2,\dots,M}$ and each protein sequence \mathcal{P}_i contains a residue set $\{r_j\}_{j=1,2,\dots,N}$; Message computation function F_{MESSAGE} that outputs an d dimensional message; $\text{COMBINE}(\cdot)$ and $\text{CONCAT}(\cdot)$ operators.

Output: Protein embeddings $\{\mathbf{Z}_i\}_{i=1,2,\dots,M}$

```

1  $\mathbf{H}_i \leftarrow \text{PLMENCODER}(\mathcal{P}_i)$ 
2  $\mathbf{X}_i \leftarrow \Phi^{\text{OH}}(\{r_j\}_{j=1,2,\dots,N}) / \Phi^{\text{PLM}}(\{r_j\}_{j=1,2,\dots,N})$ 
3  $\hat{\mathbf{X}}_i \leftarrow \mathbf{X}_i \odot \Phi^{\text{POS}}$ 
4  $\mathbf{R}_i^{(0)} \leftarrow \hat{\mathbf{X}}_i$ 
5 for  $\ell = 1, 2, \dots, L_r$  do
6   for  $i = 1, 2, \dots, N$  do
7      $\mathbf{R}_i^{(\ell)} \leftarrow \text{NODEFORMER}(\mathbf{R}_i^{(\ell-1)})$ 
8   end
9 end
10  $\mathbf{R}_i \leftarrow \mathbf{R}_i^{(L_r)}$ 
11  $\mathbf{H}_i^{(0)} \leftarrow \mathbf{H}_i$ 
12 for  $\ell = 1, 2, \dots, L_p$  do
13    $\{S_j\}_{j=1,2,\dots,k} \sim \mathcal{M}$ 
14   for  $i = 1, 2, \dots, M$  do
15     for  $j = 1, 2, \dots, k$  do
16        $\mathbf{d}_{ij} = \text{COMBINE}(\mathbf{R}_i - \mathbf{R}_{S_j})$ 
17     end
18      $\hat{\mathbf{H}}_i^{(\ell)} = \text{COMBINE}(\{F_{\text{MESSAGE}}(i, j, \mathbf{H}_j^{(\ell)}, \mathbf{d}_{ij})\}_{j=1,2,\dots,k}) \mathbf{H}_i^{(\ell+1)} = \text{CONCAT}(\mathbf{H}_i^{(\ell)}, \hat{\mathbf{H}}_i^{(\ell)}) \mathbf{W}^\ell$ 
19   end
20 end
21  $\mathbf{Z}_i^{\text{P}} = \mathbf{H}_i^{(L_p)}$ 
22  $\mathbf{Z}_i^{\text{R}} = \text{MEAN POOL}(\mathbf{R}_i)$ 
23  $\mathbf{Z}_i = \text{CONCAT}(\mathbf{Z}_i^{\text{P}}, \mathbf{Z}_i^{\text{R}})$ 

```

We summarise the process of Evolution-aware Message Passing Neural Network (EVOLMPNN) in Algorithm 1. Given a protein set $\mathcal{M} = \{\mathcal{P}_i\}_{i=1,2,\dots,M}$ and each protein sequence \mathcal{P}_i contains a residue set $\{r_j\}_{j=1,2,\dots,N}$. For each protein \mathcal{P}_i , we first initialise protein sequence (\mathbf{H}_i) and residue embeddings (\mathbf{X}_i) (line 1-2). After, the residue embeddings are empowered with positional encoding (Φ_{POS}) to get $\hat{\mathbf{X}}_i$ (line 3). Such a design will help us to record the position of a mutation occurring in the protein sequence in the following steps. Then, we update residue embedding based on a contact map, which records the chemical reactions between residues after folding into a 3D structure (line 4-10). Furthermore, we aggregate evolution-aware embeddings by means of updated residue embeddings (line 11-17) and integrate them with protein sequence embeddings to empower them with evolution-aware semantics (line 18-21). Finally, we merge protein sequence and residue embeddings as the final protein embeddings, which contain comprehensive information and make predictions based on them (line 22- line 23).

B Theoretical Analysis

Inspired by [52], we adopt Bourgain’s Theorem [53] to guide the random anchor number (k) of the evolution encoding layer, such that the resulting embeddings are guaranteed to have low distortion. Specifically, distortion measures the faithfulness of the embeddings in preserving distances (in our case, is the differences between protein sequences on a homology network) when mapping from one metric space to another metric space, which can be defined as:

Definition 1 (Distortion). *Given two metric space $(\mathcal{M}, F_{\text{DIST}})$ and $(\mathcal{Z}, F'_{\text{DIST}})$ and a function $f : \mathcal{M} \rightarrow \mathcal{Z}$, f is said to have distortion α , if $\forall \mathcal{P}_i, \mathcal{P}_j \in \mathcal{M}$, $\frac{1}{\alpha} F_{\text{DIST}}(\mathcal{P}_i, \mathcal{P}_j) \leq F'_{\text{DIST}}(f(\mathcal{P}_i), f(\mathcal{P}_j)) \leq F_{\text{DIST}}(\mathcal{P}_i, \mathcal{P}_j)$.*

Theorem 1 (Bourgain Theorem). *Given any finite metric space $(\mathcal{M}, F_{\text{DIST}})$, with $|\mathcal{M}| = M$, there exists an embedding of $(\mathcal{M}, F_{\text{DIST}})$ into \mathbb{R}^k under any l_p metric, where $k = O(\log^2 M)$, and the distortion of the embedding is $O(\log M)$.*

Theorem 1 states the Bourgain Theorem [53], which shows the existence of a low distortion embedding that maps from any metric space to the l_p metric space.

Theorem 2 (Constructive Proof of Bourgain Theorem). *For metric space $(\mathcal{M}, F_{\text{DIST}})$, given $k = \log^2 M$ random sets $\{S_j\}_{j=1,2,\dots,\log^2 M} \subset \mathcal{M}$, S_j is chosen by including each point in \mathcal{M} independently with probability $\frac{1}{2^j}$. An embedding method for $\mathcal{P}_i \in \mathcal{M}$ is defined as:*

$$f(\mathcal{P}_i) = \left(\frac{F_{\text{DIST}}(\mathcal{P}_i, S_1)}{k}, \frac{F_{\text{DIST}}(\mathcal{P}_i, S_2)}{k}, \dots, \frac{F_{\text{DIST}}(\mathcal{P}_i, S_{\log^2 M})}{k} \right), \quad (9)$$

Then, f is an embedding method that satisfies Theorem 1.

Anchor Selection. EVOLMPNN can be viewed as a generalisation of the embedding method of Theorem 2 [54], where $F_{\text{DIST}}(\cdot)$ is generalised via message passing functions (Eq 3-Eq. 6). Therefore, Theorem 2 offers a theoretical guide that $O(\log^2 M)$ anchors are needed to guarantee low distortion embedding. Following this principle, EVOLMPNN choose $k = \log^2 M$ random anchors, denoted as $\{S_j\}_{j=1,2,\dots,\log^2 M}$, and we sample each protein in \mathcal{M} independently with probability $\frac{1}{2^j}$.

C Datasets

Adeno-associated virus (AAV) capsid proteins are responsible for helping the virus carrying viral DNA into a target cell [61]; there is great interest in engineering versions of these proteins for gene therapy [14, 62, 63]. [14] produces mutants on a 28 amino-acid window from position 561 to 588 of VP-1 and measures the fitness of resulting variants with between 1 and 39 mutations. We adopt three splits from the benchmark [4], including 2-VS-REST, 7-VS-REST and LOW-VS-HIGH.

GB1 is the binding domain of protein G, an immunoglobulin binding protein found in Streptococcal bacteria [64, 65]. [16] measure the fitness of generated mutations. We adopt three splits from the benchmark [4], including 2-VS-REST, 3-VS-REST and LOW-VS-HIGH.

The green fluorescent protein is an important marker protein, enabling scientists to see the presence of the particular protein in an organic structure by its green fluorescence [66]. [15] assess the fitness of green fluorescent protein mutants. We adopt one available split, 3-VS-REST, from the benchmark [5]. Besides, in order to evaluate the models' effectiveness, we add two splits, 2-VS-REST and LOW-VS-HIGH, in this paper.

D Baselines

We present details about our baseline and proposed models in Table 4.

Table 4: Description and implementation of baseline methods.

Method	Description	Encoder	Pooling	Output layer
Levenshtein	Levenshtein distance to wild-type.	-	-	-
BLOSUM62	BLOSUM62-score relative to wild-type.	-	-	-
DDE	ipeptide Deviation from Expected Mean	2-layer MLP	-	-
Moran	Moran correlation	2-layer MLP	-	-
LSTM	Simple LSTM model	3-layer LSTM	Weighted sum pool	2-layer MLP
Transformer	Simple Transformer model	4-layer Transformer, 4 attention heads	-	2-layer MLP
CNN	Simple convolutional model	2-layer CNN	Max pool	2-layer MLP
ResNet	Classic framework of skip connections and residual blocks	8-layer ResNet	Attentive weighted sum	2-layer MLP
ProtBert	750M param transformer pre-trained on Uniref 50	30-layer BERT 16 attention heads	Linear pool	2-layer MLP
ESM-1b	650M param transformer pre-trained on Uniref 50	-	Mean pool	2-layer MLP
ESM-1v	650M param transformer pre-trained on Uniref 90	-	Mean pool	2-layer MLP
ESM-2	3B param transformer pre-trained on Uniref 50	-	Mean pool	2-layer MLP
GCN	Graph convolutional network	2/3-layer GCN encoder	-	2-layer MLP
GAT	Graph attention network	2/3-layer GAT encoder	-	2-layer MLP
GraphTransf.	Transformer model designed for graphs	2/3-layer GraphTransf. encoder	-	1-layer MLP
Nodeformer	Efficient Transformer variant design for graphs	2/3/4-layer Nodeformer encoder	-	1-layer MLP
EVOLMPNN	-	2/3-layer Residue encoder and Evolution encoder	-	1-layer MLP
EVOLGNN	-	2/3-layer Residue encoder and Evolution encoder	-	1-layer MLP
EVOLFORMER	-	2/3-layer Residue encoder and Evolution encoder	-	1-layer MLP